A Limited In-Flight Evaluation of the Constant Current Loop Strain Measurement Method

Candida D. Olney and Joseph V. Collura
NASA Dryden Flight Research Center
Edwards, California

1997

A LIMITED IN-FLIGHT EVALUATION OF THE CONSTANT CURRENT LOOP STRAIN MEASUREMENT METHOD

Candida D. Olney* and Joseph V. Collura[†]
NASA Dryden Flight Research Center
Edwards, California

Abstract

For many years, the Wheatstone bridge has been used successfully to measure electrical resistance and changes in that resistance. However, the inherent problem of varying lead wire resistance can cause errors when the Wheatstone bridge is used to measure strain in a flight environment. The constant current loop signal-conditioning card was developed to overcome that difficulty. This paper describes a limited evaluation of the constant current loop strain measurement method as used in the F-16XL ship 2 Supersonic Laminar Flow Control flight project. Several identical strain gages were installed in close proximity on a shock fence which was mounted under the left wing of the F-16XL ship 2. Two strain gage bridges were configured using the constant current loop, and two were configured using the Wheatstone bridge circuitry. Flight data comparing the output from the constant current loop configured gages to that of the Wheatstone bridges with respect to signal output, error, and noise are given. Results indicate that the constant current loop strain measurement method enables an increased output, unaffected by lead wire resistance variations, to be obtained from strain gages.

Nomenclature

A	gain
E	excitation voltage across the bending bridge, volts
E_{omax}	maximum expected voltage output of the gage, volts
GF	gage factor
I	current, ampere
PCM	pulse code modulator
R_g	resistance of strain gage $\ldots$ n^{th}, ohms
ΔR_g	change in resistance in strain gage $\ldots$ n^{th}, ohms
R_{ref}	resistance of the reference strain gage, ohms
R_w	resistance of lead wire $\ldots$ n^{th}, ohms
SLFC	Supersonic Laminar Flow Control
V_a	voltage drop across inboard strain gages, volts
V_b	voltage drop across outboard strain gages, volts
V_g	voltage drop across strain gage $\ldots$ n^{th}, volts
V_{out}	voltage output, volts
V_{out_g}	voltage output of the strain gage $\ldots$ n^{th}, volts

---

* Aerospace Engineer, Aerostructures Branch, 805-258-3988
[†] Electrical Engineer, Instrumentation Branch, 805-258-2814

V_{PCMmax} maximum allowable voltage input to the PCM, volts

Vrms root mean square voltage

β angle of sideslip, deg

ε strain, $\mu in/in$

ε_{max} expected maximum strain, $\mu in/in$

$\mu in/in$ microstrain, $10^{-6} in/in$

Introduction

For many years, strain gage instrumentation has been used to measure strain within structural components. Traditionally, these strain gages were configured using the Wheatstone bridge circuit. However, the output of Wheatstone bridges is susceptible to varying lead wire resistance because of temperature effects, lead wire gauge, and wire length. These variations may decrease the sensitivity of the strain gage to strain inputs (ref. 1).

A constant current loop strain measurement method was developed by NASA Dryden Flight Research Center (DFRC), Edwards, California, and patented by Karl F. Anderson (ref. 2) to overcome the difficulties associated with the Wheatstone bridge. This constant current loop strain measurement method consists of the strain gages, constant current loop signal-conditioning card, pulse code modulator (PCM), and signal transmitter. The constant current loop signal-conditioning card uses a constant current source in conjunction with strain gages to measure strain.

This signal-conditioning card was initially tested in the Thermostructural Research Facility (ref. 3).* During these laboratory tests before flight, Wheatstone bridge signal conditioning was replaced with the constant current loop signal conditioning.

Results indicated that the constant current loop strain measurements were insensitive to lead wire resistance changes and were accurate when connected to a strain indicator calibration standard. However, data comparisons between the Wheatstone bridge and the constant current loop strain measurement systems were not made.

Flight tests were performed to compare the strain gage outputs using the constant current loop and Wheatstone bridge strain measurement methods in a flight environment. The constant current loop strain measurement system was flight tested using three different lead wire configurations: seven-, five-, and three-wire configurations. Diagrams of these three configurations are presented in appendix A. The seven-wire configuration allows individual gage measurements to be made. All three configurations were used to obtain strain outputs from four-active-arm-bending bridges.

This paper presents a comparison of the Wheatstone bridge and constant current loop signal-conditioning methods and a description of the experimental method. In addition, a comparison of the data collected during flights 87 and 88 of the F-16XL ship 2 Supersonic Laminar Flow Control (SLFC) project using the Wheatstone bridge and the constant current loop strain measurement methods is given. Use of trade names or names of manufacturers in this document does not constitute an official endorsement of such products or manufacturers, either expressed or implied, by the National Aeronautics and Space Administration.

---

*The name of the DFRC Thermostructural Research Facility was changed to the Flight Loads Laboratory in 1996.

2

Aircraft Configuration

The constant current loop signal-conditioning card was installed as a secondary experiment on the F-16XL ship 2 SLFC project (ref. 4) (fig. 1). The SLFC experiment was designed to produce laminar flow over a gloved test section on the left wing of the modified F-16XL ship 2 by using active suction through the glove to remove the boundary layer during supersonic flight. It was determined that during supersonic flight, a shock wave from the engine inlet distorts the flow on the leading edge of the wing. A shock fence (fig. 2) was installed under the wing to prevent the shock wave from interfering with the airflow over the wing.

Figure 3 shows an overall view of the inboard surface of the shock fence and the relative positions of the strain gages. Two sets of prime and spare four-active-arm-bending bridges were installed on the shock fence in the areas of the maximum predicted strain. The prime and spare strain gages were located in close proximity to each other and originally were wired in a Wheatstone bridge configuration. One set was located at a forward location on the shock fence, and one was installed at an aft location. To perform a flight evaluation, the signal-conditioning cards for the spare Wheatstone bridges were replaced with constant current loop cards.

The spare strain gages at the forward location were re-wired in the constant current loop seven-lead-wire configuration. The output from the seven-wire configuration was used to create output for the five- and three-wire configurations. The wiring for the spare strain gages at the aft location were configured using five lead wires. These configurations allowed comparisons of the output of the two strain measurement systems to be made.
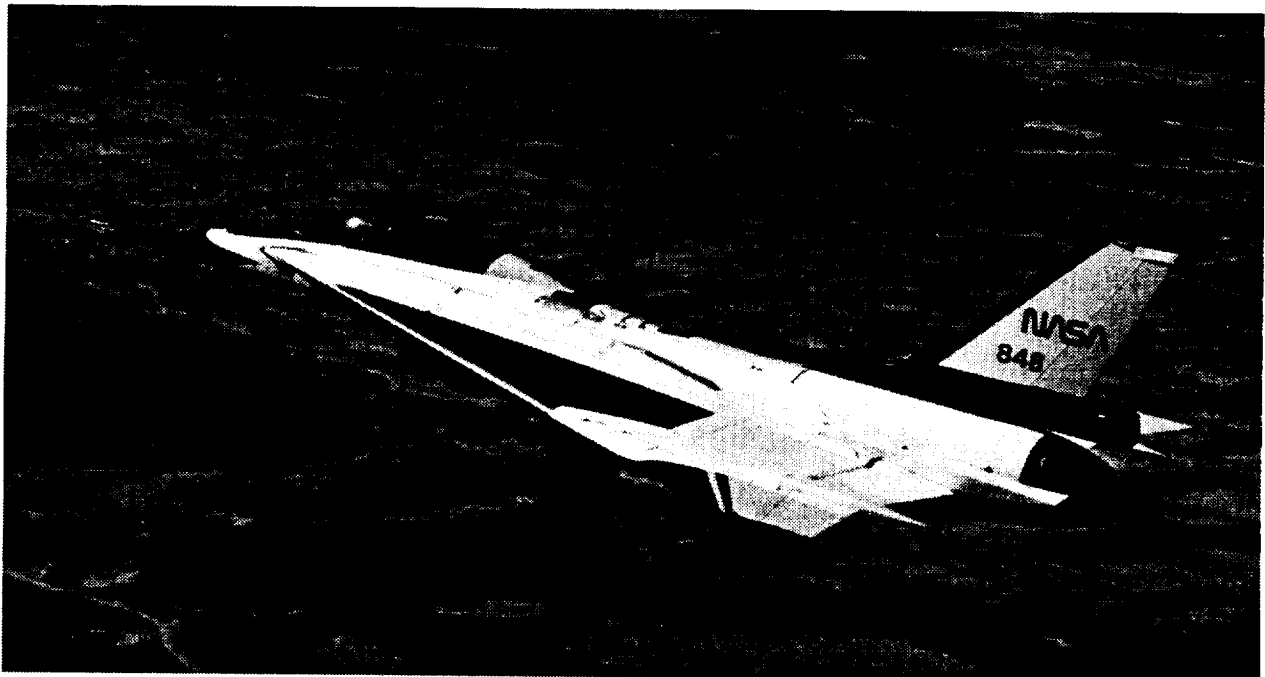
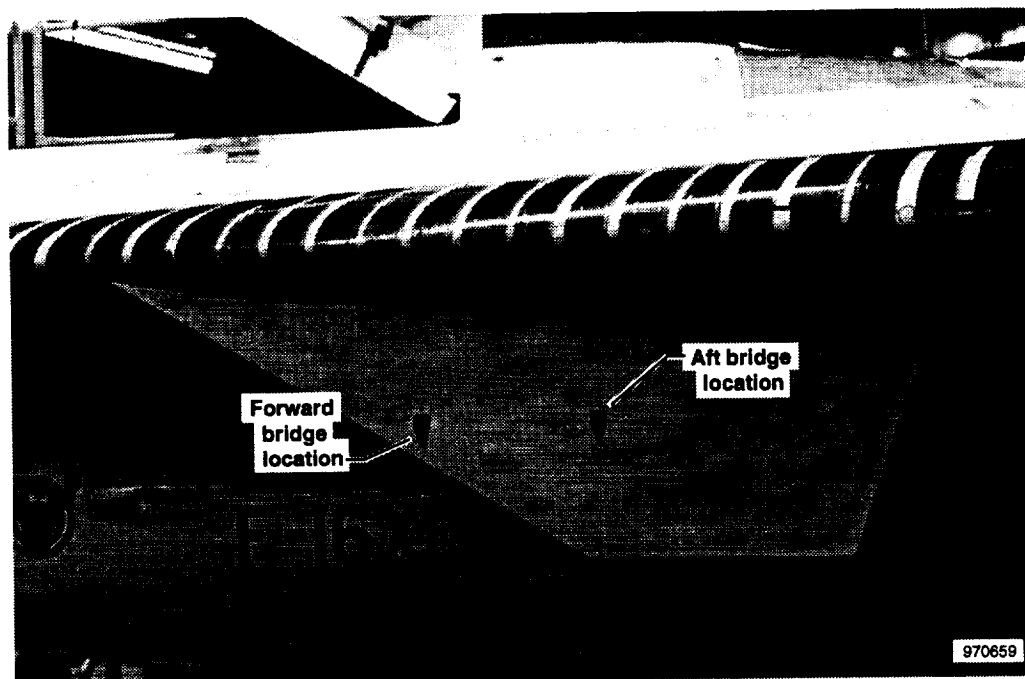EC95 43297-07

Figure 1. The F-16XL ship 2.
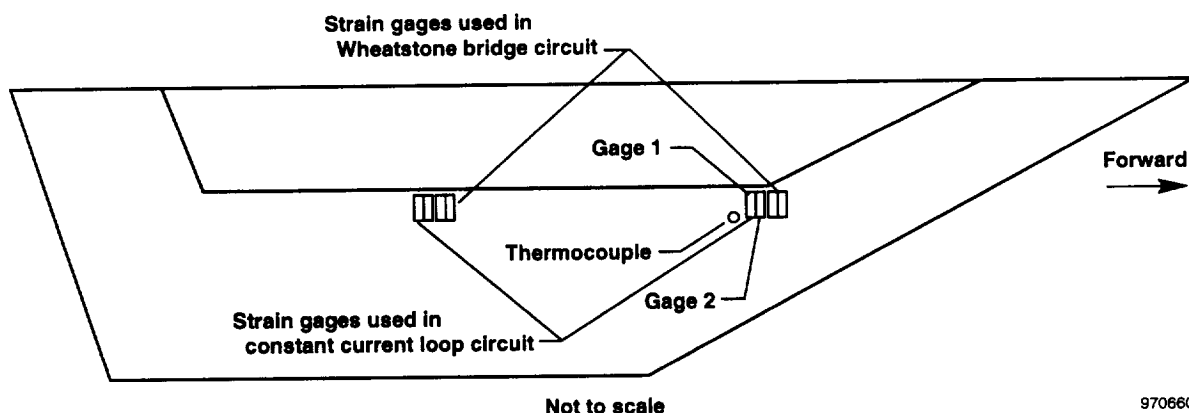
3

Figure 2. The F-16XL ship 2 shock fence.

Figure 3. Inboard surface of the shock fence with strain gages installed.

Description of Wheatstone Bridge and Constant Current Loop Signal Paths

Figure 4 shows the signal path for all of the strain measurement systems. After excitation is applied to the strain gages, the signal is carried to the signal-conditioning cards and processed. The signal then is sent to the PCM and is downlinked to the ground station. Several significant differences exist between the signal paths of the constant current loop and the Wheatstone bridge strain measurement systems. These differences include the gage excitation method, number of lead wires required, signal-conditioning process, and wiring to the PCM.

Excitation Methods

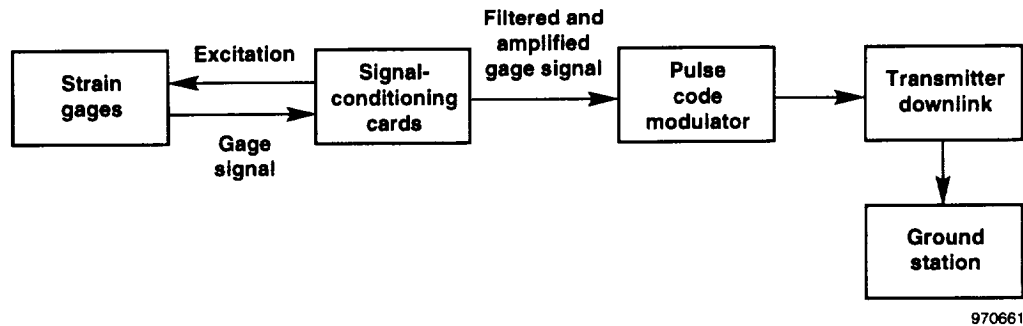The excitation methods are fundamentally different for the two measurement systems.

4

Figure 4. Instrumentation signal path for strain gage measurements.

The Wheatstone bridge method uses a constant voltage source for the excitation of the strain gages. The Wheatstone bridge signal-conditioning applies 10 volts across the bridge, which results in 5 volts across the individual gages. A diagram of the Wheatstone bridge circuit used in this experiment is presented in appendix A. As the lead wire resistances increase, the voltage potential across the gages drops, thereby causing a reduced effective excitation voltage. Therefore, the sensitivity of the Wheatstone bridge to strain changes decreases when the lead wire resistances increase.

As the name implies, the constant current loop signal-conditioning card uses constant current regulation to provide gage excitation. The regulator compares a stable 5-volt source with the voltage across the reference resistor in its current loop (ref. 3). Because the reference resistor is physically located on the signal-conditioning card, it does not experience the same environmental conditions that the strain gages experience. Therefore, the resistance of the reference resistor is constant. The return current input into the circuit is adjusted by the regulator so that a stable, constant current is applied to the strain gages.

Lead Wires

Another difference between the constant current loop and Wheatstone bridge configurations is the number of lead wires required. The two Wheatstone bridges each had four lead wires contained in shielded, four-wire bundles. This approach causes the lead wires to experience essentially the same environment so that their resistances change consistently. If the lead wires do not change the same, then the strain measurements will not be accurate (ref. 5). However, even if the lead wire resistances do increase equally, the sensitivity of the strain gages to a strain input is reduced by a varying amount which is difficult to quantify.

The constant current loop strain gages were arranged with three different lead wire configurations for this experiment. These three configurations use seven, five, and three lead wires. In this application, the forward constant current loop strain gages were wired in the seven-lead-wire configuration. The five- and three-lead-wire configurations were created on the signal-conditioning card by jumpering the signals at the appropriate points. Appendix A gives a derivation of the outputs of the constant current loop strain gages and explains how

5

data from the five- and three-lead-wire configurations were obtained.

The seven lead wires were included in a shielded, eight-wire bundle, thereby leaving one wire unused. The aft constant current loop gages were configured using five lead wires contained in a shielded, six-wire bundle. The derivation in appendix A reveals that no assumptions need to be made about the lead wire resistance changes in the seven- and five-lead-wire configurations. However, when the three-lead-wire configuration is used, the assumption must be made that the two current-carrying lead wires will change equally. As with the Wheatstone bridge configuration, this assumption is valid as long as the current-carrying lead wires experience the same environment. However, unlike the Wheatstone bridge, a change in the lead wire resistances does not affect the output of the constant current loop.

Signal-Conditioning Cards

The outputs of the strain gages are sent to their respective signal-conditioning cards. The signal-conditioning cards for the two strain measurement systems differ in the number of signal-conditioning cards required, number of measurements that these cards can accommodate, shunt resistor calibration capability, and signal-conditioning components.

The Wheatstone bridge signal conditioning in this evaluation used two cards (fig. 5(a)). Each set of two cards accommodates eight gage arrangements or bridges. The first card in the Wheatstone bridge signal path is the shunt resistor calibration card. This calibration card receives the voltage information from the full-bridge gage output. The full-bridge output may be

commanded to a simulated strain level by shunting a known resistance across one arm of the bridge. The resistor calibration card also allows for an external switch to control all of the relays. These relays simultaneously place all circuits into calibration mode.

The second Wheatstone bridge card amplifies the input signal and filters the output signal. The differential voltage across the output of the bridge is read using an instrumentation amplifier which applies the assigned gain to the signal. The output from the amplifier is then sent to the filter circuit. The filter is a third-order, active, low-pass filter which accomplishes noise reduction and presample filtering. The output of the low-pass filter is then sent to the PCM.

The bridges using the constant current loop have the signal path shown in figure 5(b). They use a single, multilayer, signal-conditioning card which can read four full-bridge strain gage measurements. These four measurements could include four of the five- or three-lead-wire bending bridges or eight individual gage measurements, which would be used in two of the seven-lead-wire bending bridges.

Unlike the Wheatstone bridge, the constant current loop strain measurement system used in this experiment did not provide the ability to externally place the strain gages into calibration mode. A shunt calibration switch was located directly on the signal-conditioning card. Therefore, aircraft panels had to be removed to perform the shunt calibration. This time consuming process can invalidate the aircraft preflight and prevent calibrations from being performed in flight.
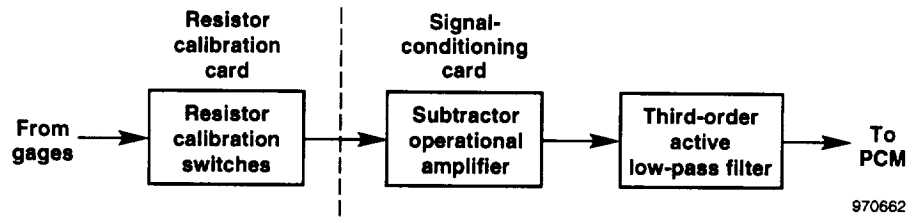
(a) Wheatstone bridge.
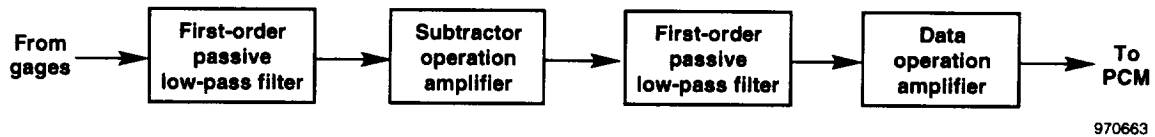
(b) Constant current loop.

Figure 5. Signal-conditioning card signal paths.

The constant current loop signal-conditioning card used provided the ability to wire the signal-conditioning card directly to a shunt calibration card. However because of the number of cards required for the constant current loop measurements, no space was available for the additional calibration card. For example, to externally put eight full bridges into calibration mode, the constant current loop method requires three cards; meanwhile, the Wheatstone bridge requires two. To measure the voltage output from these strain gages, the constant current loop signal-conditioning card was equipped with eight input instrumentation amplifiers for use as subtractors and eight output instrumentation amplifiers to provide the gain.

Figure 5(b) shows the relationship of filters and amplifiers for the constant current loop, and appendix A shows the placement of the amplifiers within the circuit. The output signal from the strain gage is routed through a first-order, passive, low-pass filter to the input of the subtractor instrumentation amplifier. When using the five- and three-lead-wire configurations, two instrumentation amplifiers are needed to take readings across both sides of the bridge.

However, in the seven-lead-wire configuration, one subtractor is required for reading the voltage drop across each gage. Output of the subtractor stage is then sent to another instrumentation amplifier whose input is filtered with another first-order, passive, low-pass filter. This instrumentation amplifier, or data amplifier, is responsible for amplifying its input signal from either one or two subtractors to the level required by the PCM system input. The constant current loop signal-conditioning card does not use a filter after the data amplifiers.

Wiring from Signal-Conditioning Card to PCM

Wiring schemes from the Wheatstone bridge and constant current loop signal-conditioning cards to the PCM differ in the number of data amplifier reference lines that are tied together at each of the signal-conditioning cards. One PCM analog

7

module has 16 single-ended inputs consisting of one return line for four input lines.

For each Wheatstone bridge measurement, four signal lines are sent to the PCM, and four signal returns are jumpered together in one return line to the PCM (fig. 6(a)). Conversely, for the constant current loop signal conditioning cards, all eight outputs of the card have their output returns tied together on the card. Only one line is used to carry the return voltage (fig. 6(b)).

Experimental Method

Sixteen CEA-13-250-UW-350 (Micro-Measurements, Romulus, Michigan) strain gages with a gage factor of 2.115 were used in four-active-arm-bending bridges. Two complete bending bridges each were placed in close proximity in forward and aft locations on the shock fence (fig. 3). Each bridge consisted of two active arms on the inboard surface of the shock fence and two on the outboard surface.

Figure 7 shows the forward gages installed on the inboard side of the shock fence. The
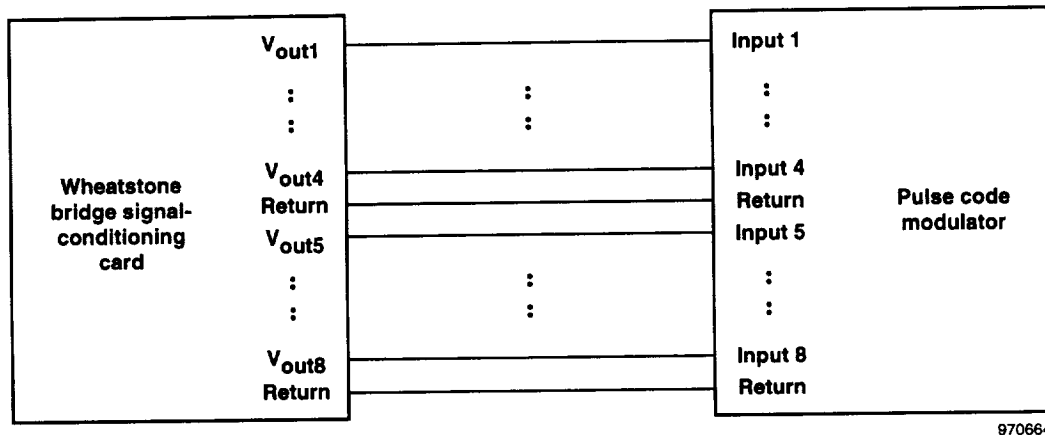
(a) Wheatstone bridge.
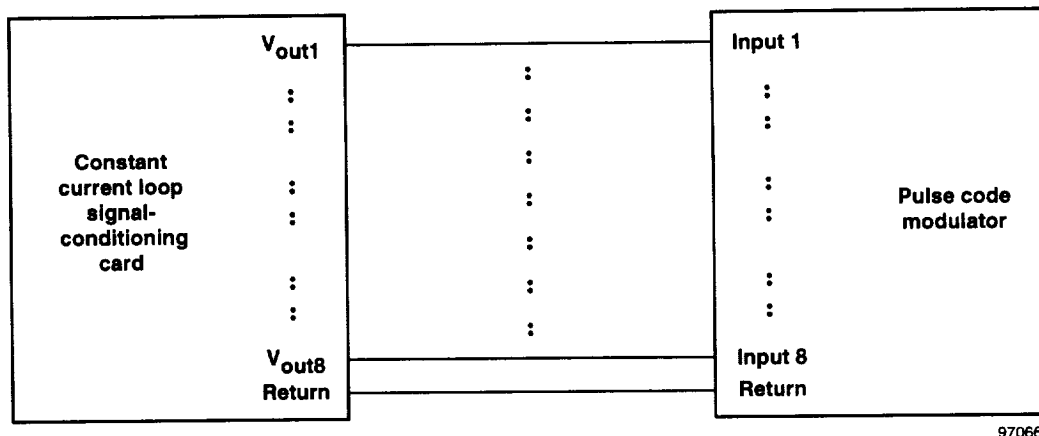
(b) Constant current loop.

Figure 6. Wiring from the signal-conditioning card to the pulse code modulator.

8

strain gages using the Wheatstone bridge circuitry are forward of the strain gages using the constant current loop in both the forward and aft locations on the shock fence. A thermocouple was installed aft of the constant current loop configured strain gages in the forward location to measure the temperature of the shock fence during the test flights. Data from the thermocouple are presented in appendix B.

The forward constant current loop bridge was wired using the seven-lead-wire configuration. However, during the flight, five- and three-lead-wire measurements were made concurrently at the forward location. These simultaneous measurements were made by jumpering the signals at the appropriate locations on the constant current loop signal-conditioning card (appendix A).

To properly scale the outputs from the constant current loop strain gages, the gain for the data amplifier was based upon the maximum strain level seen in previous flights. The maximum strain output was 262 μin/in. Therefore, the strain scale for the gage output was set to ±300 μin/in to maximize the data resolution while preventing the signals from going off scale. Equation (1) gives the method used to determine the maximum output for a single gage.

$$E_{omax} = GF \times \varepsilon_{max} \times E \qquad (1)$$

Because E is set equal to the maximum input of the PCM, 5 V, the gage factor is 2.115 and ε_{max} is equal to 300 μin/in, the maximum output from one strain gage, E_{omax}, is 3 mV. The next step is to correlate the maximum expected output from the strain gage with the maximum allowable input for the PCM. This
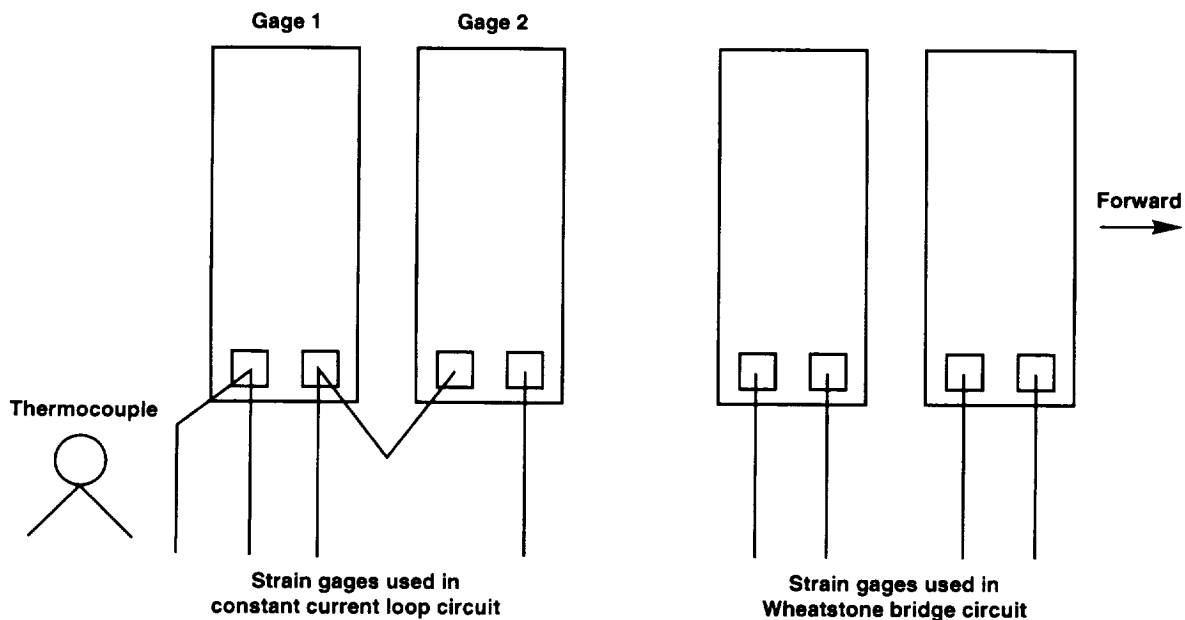
Figure 7. The strain gages and thermocouple installed on the inboard surface of the shock fence at the forward location.

9

correlation factor is called the gain. The gain, A, is calculated by

$$A = \frac{V_{PCMmax}}{E_{omax}} \qquad (2)$$

Because the input range for the PCM is ±5 V, the gain for the individual gages is calculated to be 1667. The output from the four-gage bridge circuit is four times higher than that of the individual gages. Therefore, the gains for the complete bridges are reduced by a factor of 4, and the gain for the bending bridge measurements is 417. The gain on the Wheatstone bridge signal-conditioning card was set equal to the gain on the constant current loop signal-conditioning card to compare the signal-to-noise ratios.

Strain measurements were made at the forward and aft locations throughout the entire flight (fig. 3). However, because the shock fence was expected to experience the maximum strain when the angle of sideslip, β, reached its maximum value, it was decided that the strain measurements would be compared using data taken while the aircraft completed three 5° nose-left and nose-right β sweeps.

This maneuver was performed shortly after takeoff during the phasing maneuvers at approximately 5000 ft and Mach 0.7. The phasing maneuvers are performed to ensure that the aircraft instrumentation functions properly. Because of the nature of the primary experiment, no maneuvers were performed while the aircraft was flying supersonically. Therefore, data comparisons were not made while the aircraft was experiencing elevated temperatures. Data were taken while shock fence temperatures ranged between 100 °F and −40° F.

Results and Discussion

Because data from the forward strain gages were similar to that obtained for the aft strain gages, only data from the forward strain gages are presented in this paper. Appendix B includes graphs of the aircraft flight conditions, such as Mach number, dynamic pressure, shock fence temperature, angle of attack, and angle of sideslip, which correlate to the strain graphs presented in this paper.

Figure 8(a) shows the strains measured from all of the configurations of the forward strain gages while the aircraft completed three β sweeps during flight 88. All three of these constant current loop lead wire configuration strains closely follow the strain measured by the Wheatstone bridge. Figure 8(b) shows the differences between these signals. In this figure, the output from the Wheatstone bridge was subtracted from the total output of each of the constant current loop lead-wire configurations. Table 1 lists the results.
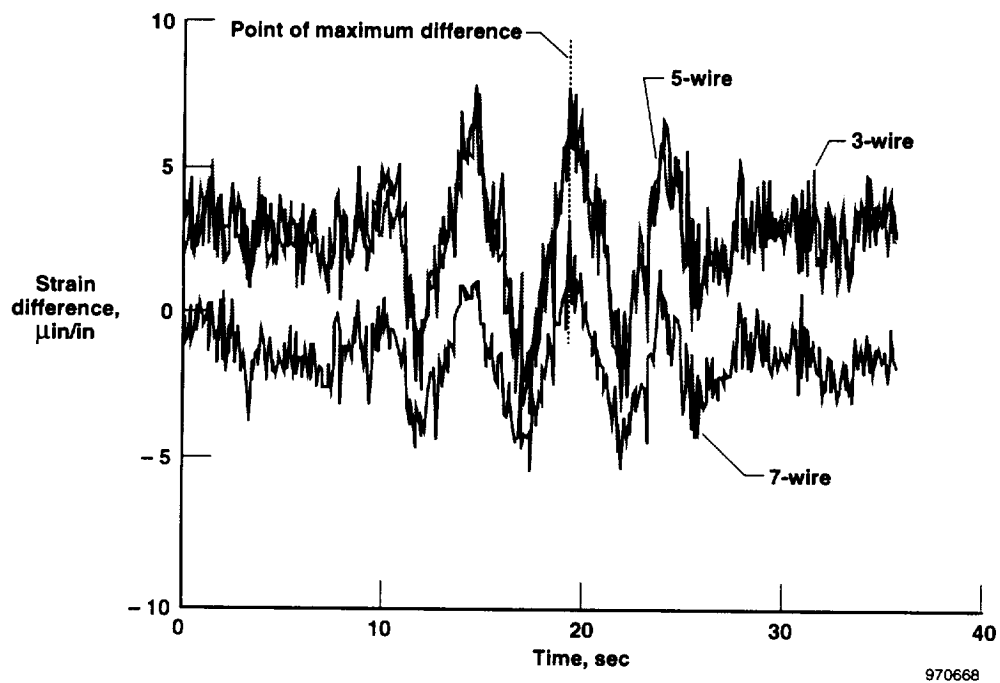
Table 1. Differences between constant current loop and Wheatstone bridge strain measurements during phasing maneuvers.

Constant current loop lead wire configurations	Maximum, μin/in	Standard deviation, μin/in
7	5.6	1.5
5	7.7	2.1
3	7.3	2.0

The five- and three-lead-wire configurations responded to the load similarly; meanwhile, the seven-lead-wire configuration gave a smaller response to the load. However
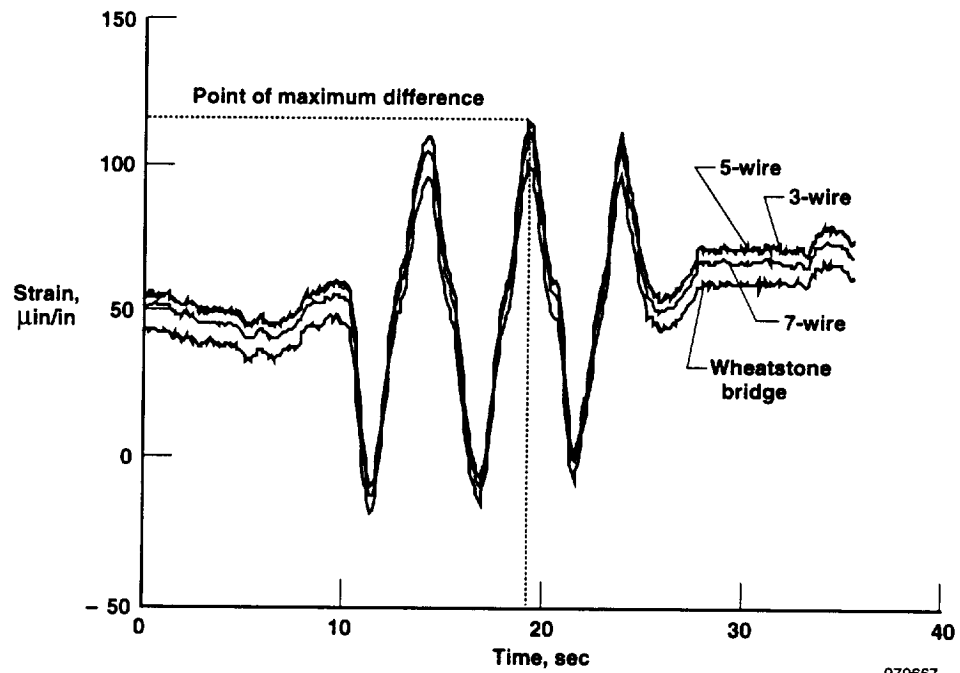
(a) Forward location.

(b) Constant current loop gage responses minus Wheatstone bridge response.

Figure 8. Strain during phasing maneuvers.

11

because the noise level of the constant current loop is approximately 1.7 μin/in, this difference is within the noise level of the data channel. Before the β sweeps, the differences between the constant current loop measurements and the Wheatstone bridge measurements were smaller. Table 2 shows these differences in responses while the aircraft is flying straight and level.

Table 2. Differences between constant current loop and Wheatstone bridge strain measurements during straight and level flight.

Constant current loop lead wire configurations	Maximum, μin/in	Standard deviation, μin/in
7	3.9	0.93
5	5.0	0.94
3	5.2	0.93

Comparing the data from tables 1 and 2 reveals that while performing the β sweeps the differences between the responses from the strain measurement systems increased slightly. These changes in the strain differences and standard deviations indicate an actual strain difference because the constant current loop and Wheatstone bridge configured strain gages were not positioned in exactly the same location.

Because the five-lead-wire constant current loop configuration did not require assumptions about the affects of temperature on the strain gages and lead wire resistances, it was used as a baseline for the constant current loop configurations. The differences in the measured strain between the constant current loop configurations were determined for the phasing maneuvers during flight 88. A graph of the differences is presented in figure 9. The averages and the standard
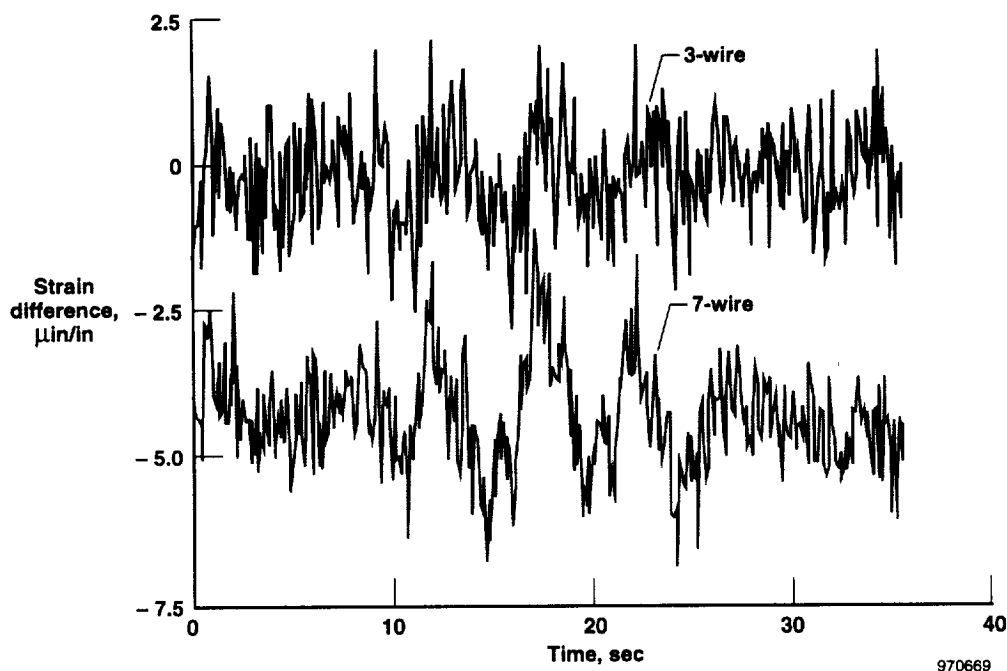

Figure 9. Strain differences between the three- and five-wire configurations and the seven- and five-wire configurations during phasing maneuvers.

12

deviations of the differences between the five-, three-, and seven-lead-wire configurations are given in table 3.

Table 3. Differences between constant current loop strain measurements during phasing maneuvers.

	Average, μin/in	Standard deviation, μin/in
3-wire minus 5-wire	0.2	0.9
7-wire minus 5-wire	4.3	1.0

There is a larger strain difference between the seven- and five-lead-wire configurations than between the three- and five-lead-wire configurations. This difference may occur because the seven-lead-wire configuration uses four data amplifiers and four data channels to record the gage outputs. Conversely, the five- and three-lead-wire configurations require two data amplifiers and one data channel each. When the individual gage responses are combined into a total bridge output for the seven-lead-wire configuration, the noise levels of each of those data channels may be added together. However in this application, the larger difference between the seven- and five-lead-wire configurations than between the three- and five-lead-wire configurations is negligible. Therefore, the three constant current loop configurations provide consistent strain gage outputs.

The total output for the constant current loop seven-lead-wire configuration was determined mathematically during postflight processing of the four individual strain gage outputs. Figure 10(a) shows the individual gage responses during the flight 88 phasing maneuvers. The
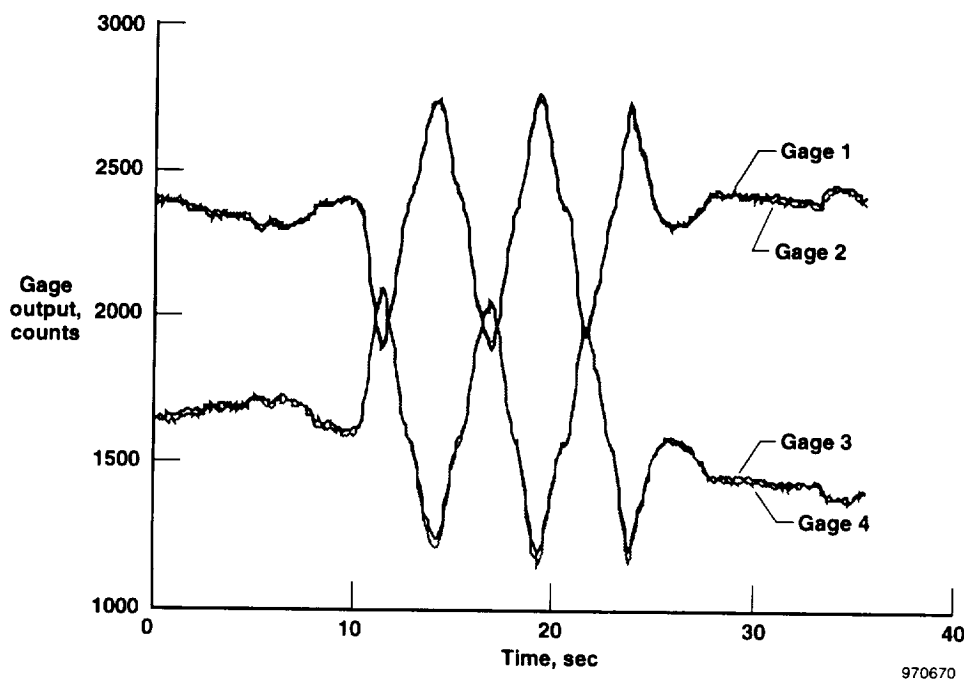
(a) Individual gage response.

Figure 10. Seven-wire configuration during phasing maneuvers.

13

responses from gages 3 and 4, which are located next to each other on the outboard surface of the shock fence, are the exact opposite of the responses from gages 1 and 2, which are located in the same position on the inboard side.

Figure 10(b) contains the summation of these individual gage responses converted to microstrain. The total bridge response of the seven-lead-wire configuration was determined by adding the strain outputs of gages 1 and 2 and subtracting the strains of gages 3 and 4. This total was then divided by 4 because the gains for the individual gages were set higher than those of the five- and three-lead-wire configurations and the Wheatstone bridge.

The seven-lead-wire configuration would be used mainly as a rosette to measure individual gage strain outputs. There is an inherent difficulty with using the seven-lead-wire configuration in this application as it was implemented in this experiment. This difficulty was demonstrated during flight 87. Because of an aircraft emergency

immediately preceding the supersonic portion of the flight, the F-16XL ship 2 was forced to return to the base at subsonic speeds. This extended subsonic run caused the shock fence to experience cold-soaking.

Graphs of the flight conditions including temperature are presented in figures B1(a) through B2(e). The strain data from the entire flight is shown in figure 11(a). Differences between the constant current loop responses and the Wheatstone bridge are shown in figure 11(b).

The summation of the individual gage responses does not accurately track with the responses from the other bridges' configurations. The responses of gages 3 and 4 from the seven-lead-wire configuration went off scale during the flight (fig. 12). A review of the manufacturer's apparent strain data revealed that this condition was caused in part by the apparent strain of the strain gages. The strain gages experience a different temperature during flight than the strain
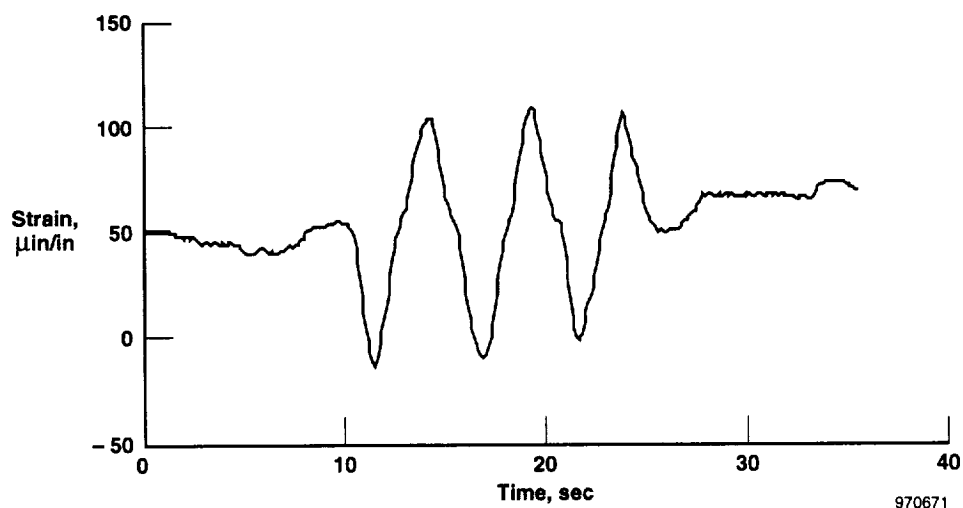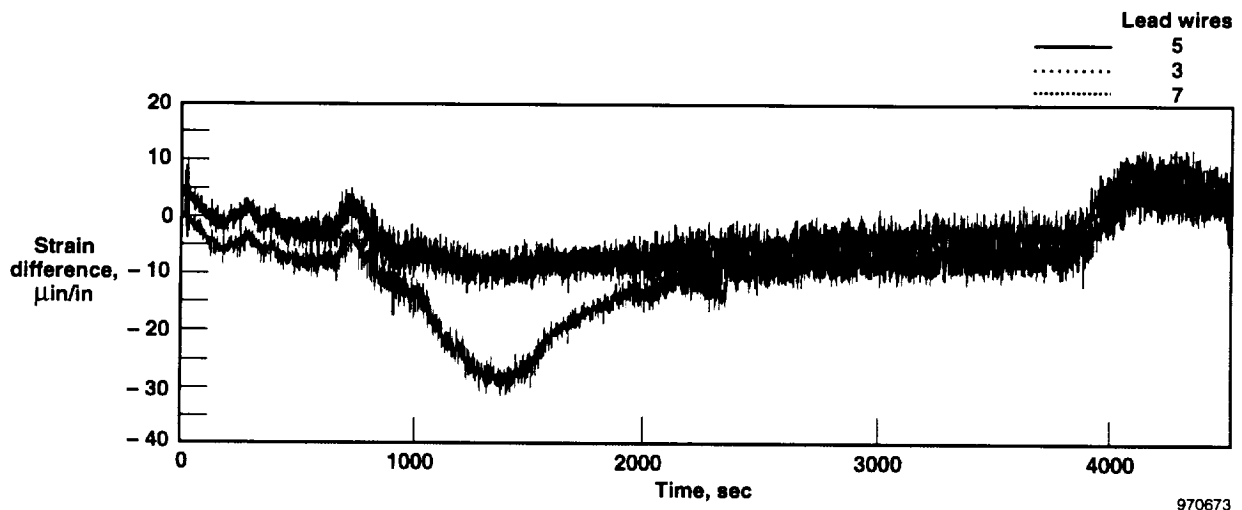

(b) Combined strain output.

Figure 10. Concluded.

14
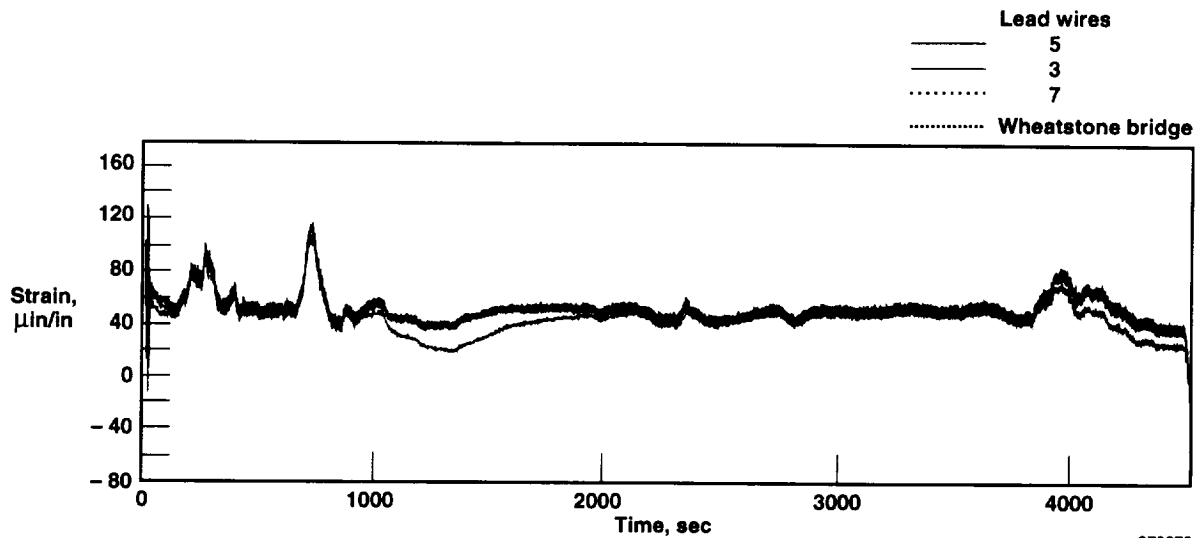
(a) Forward bridges.

(b) Differences between forward constant current loop and forward Wheatstone bridge configurations.

Figure 11. Strain during flight 87.

gage used as a reference resistance. The strain gage which is used as a reference resistance is located inside the fuselage of the aircraft. This reference resistance is used by the signal-conditioning card to subtract out the unstrained resistance of the strain gages in the seven-lead-wire configuration (appendix A).

Because it is assumed that the reference resistance is identical to the resistance of the strain gages, this temperature difference prevents the seven-lead-wire configuration from being self-compensating for apparent strain when it is used to measure individual strain gage responses. When the outputs from the individual strain
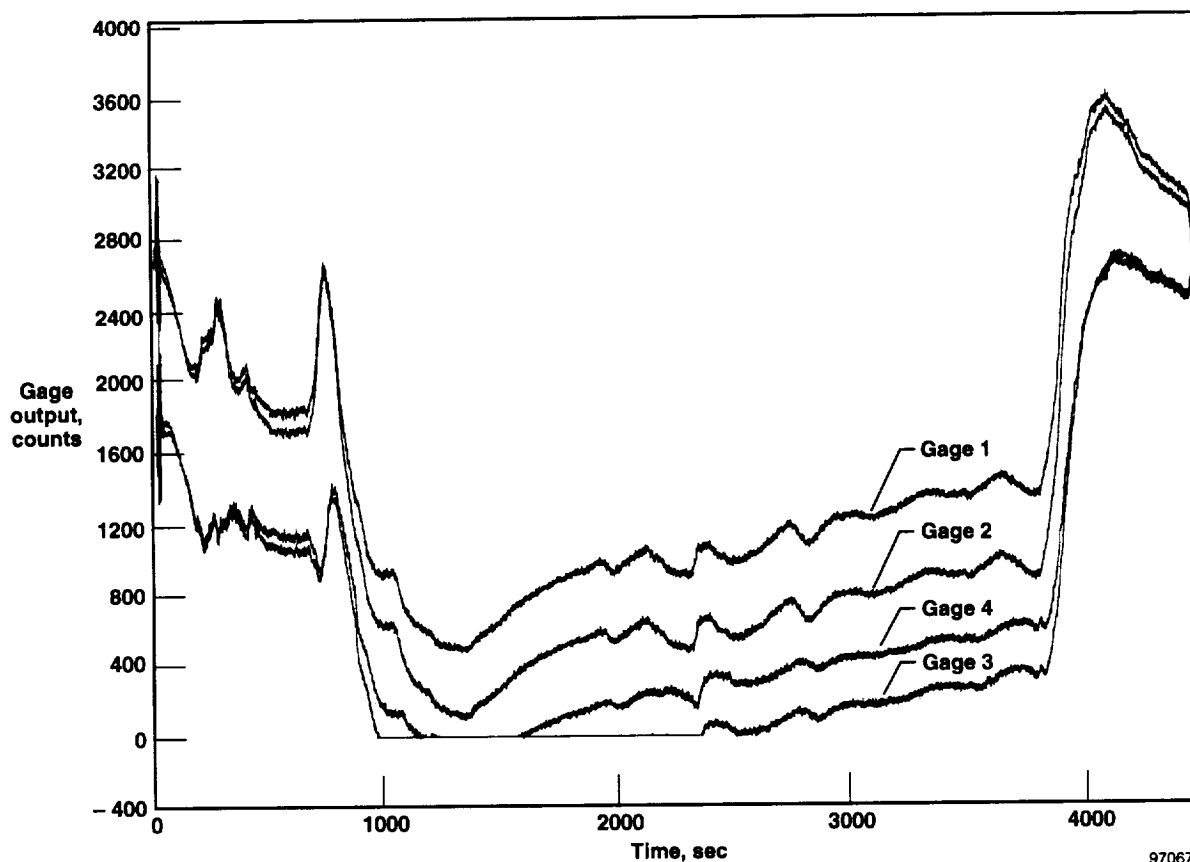
15

Figure 12. Individual gage responses from constant current loop seven-wire configuration during flight 87.

gages are mathematically summed to provide a total bridge output, this apparent strain subtracts out. Because neither the five-lead-wire nor the three-lead-wire configurations use the reference resistance to subtract out the unstrained gage resistances, their outputs are consistent. However, corrections for temperature would have to be made to the data from the seven-lead-wire configuration when it is used to measure individual strain gage outputs.

Constant Current Loop Noise Investigation

Contrary to theoretical expectations, the signal-to-noise ratio of the constant current loop signal-conditioning card was approximately the same as the Wheatstone bridge during postflight evaluation. Data presented in figures 13(a) and 13(b) were taken shortly after the aircraft had landed and while it was at rest with the engines on. These data were used as a baseline for the noise levels on the airplane. Figure 13(a) shows the noise level of the Wheatstone bridge in volts. The root mean square value of the Wheatstone bridge noise was 0.0137 Vrms. Figure 13(b) shows the noise level of gage 1 in the seven-lead-wire configuration. Gage 1 had a noise value of 0.0267 Vrms. However, the signal outputs of the constant current loop strain gages were twice as large as those of the Wheatstone bridge output.

16
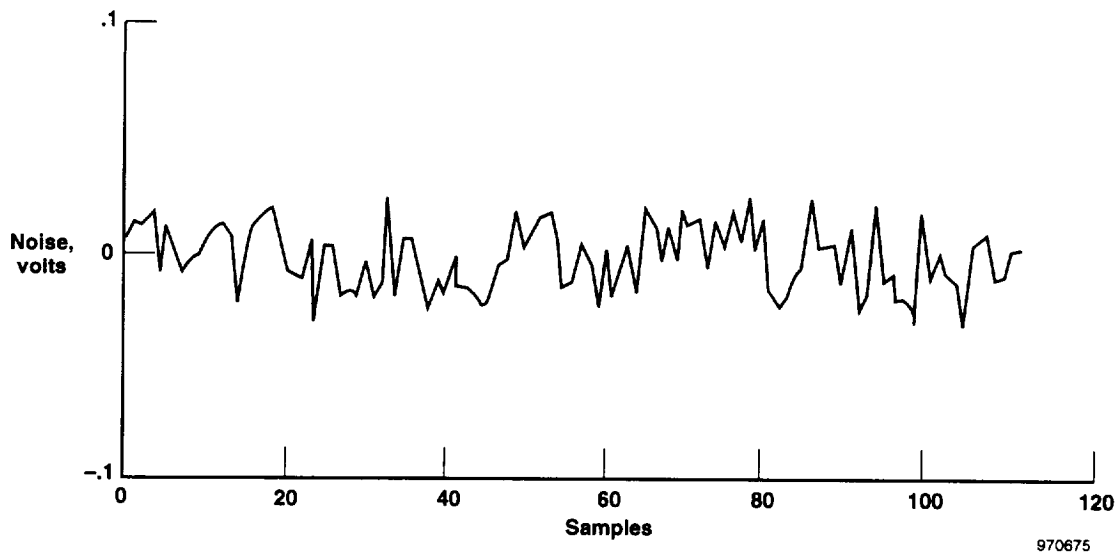
(a) Wheatstone bridge.
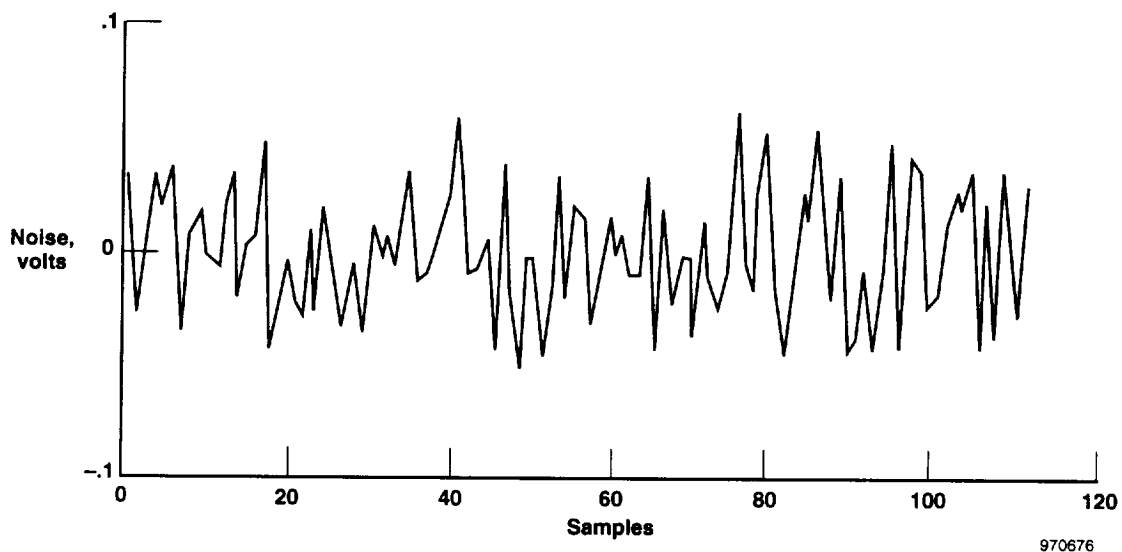
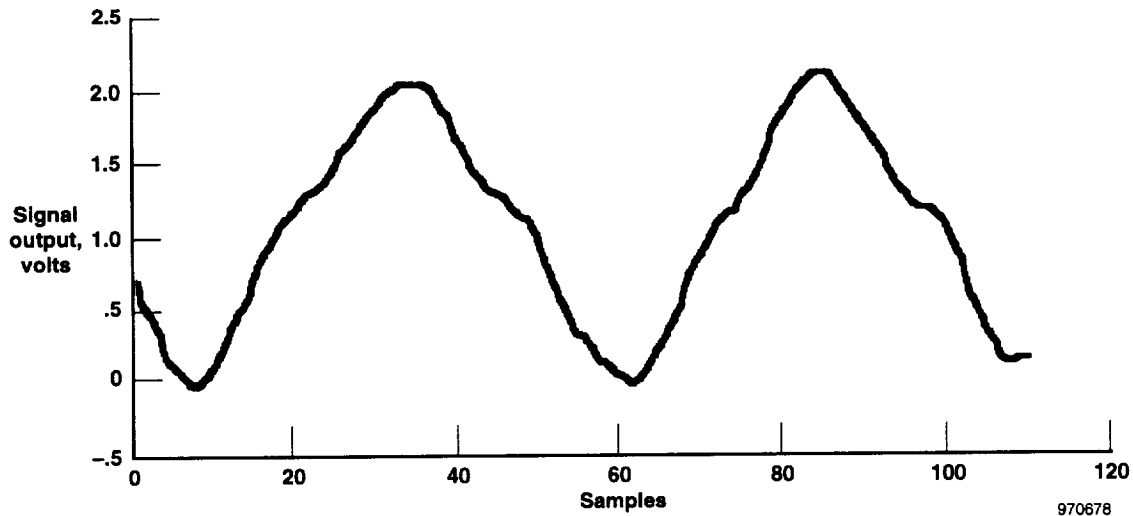(b) Gage 1 of the constant current loop configuration.

Figure 13. Noise level with direct current voltage offset removed.

Figures 14(a) and 14(b) show the signal outputs of the Wheatstone bridge and gage 1. The Wheatstone bridge signal value was 0.5 Vrms, and the constant current loop strain gage had a signal value of 1.2 Vrms. Therefore, the signal-to-noise ratios for both types of signal-conditioning cards were close to the same value.

Because theoretically, the signal-to-noise ratio of the constant current loop should be twice that of the Wheatstone bridge (ref. 6), an investigation was conducted to determine the cause of the higher than expected noise floor of the constant current loop signal-conditioning card.

17
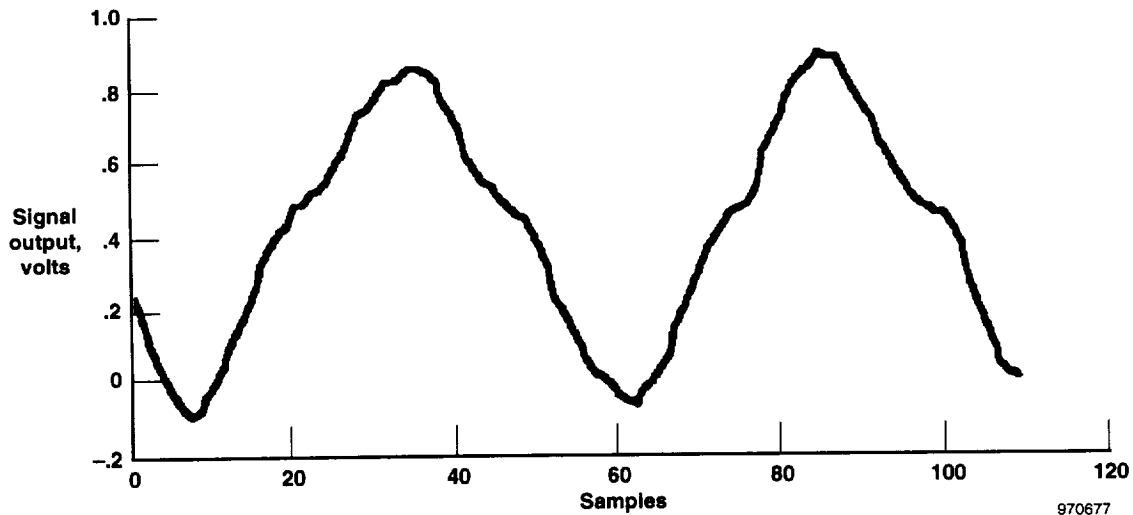
(a) Wheatstone bridge.

(b) Gage 1 of the constant current loop seven-wire configuration.

Figure 14. Signal outputs during phasing maneuvers.

Three ground tests were performed during the investigation. The output of the data amplifier was shorted showing that the excessive noise was being generated by the constant current loop signal-conditioning card. The resulting noise floor was acquired on the PCM as counts. The noise floors before and after shorting the output amplifiers are given in table 4.

Table 4. Constant current loop noise comparison test 1.

	Noise floor, Counts	Noise floor with data amplifier shorted, Counts
Mean	2146	2062
Standard deviation	12	4

18

The fact that the standard deviation decreased after the data amplifiers were shorted indicates that the data amplifiers were generating noise on the signal-conditioning card. However, this finding did not account for all of the noise being generated by the constant current loop signal-conditioning card. Further investigation was required to resolve the high noise floor problem.

After comparing the Wheatstone bridge signal-conditioning card to the constant current loop signal-conditioning card, two conditions were discovered that contribute to the high noise floor of the constant current loop signal-conditioning card. The first difference is that on the constant current loop card all eight amplifier output reference lines are tied together on the board. Therefore, only one output pin and wire are available to carry the return current back from the PCM which creates a ground loop. To test this theory, seven output amplifiers were removed from the board, and the output from a single gage measurement was taken. This change allows only the reference line of a single data channel to be connected to the PCM. Test 2 compared the noise level when all eight output amplifiers are active versus when one amplifier is active. The results are given in table 5.

Table 5. Constant current loop noise comparison test 2.

	Eight amplifiers installed, Counts	One amplifier installed, Counts
Mean	2146	2132
Standard deviation	12	7

The standard deviation for the one amplifier configuration shows that when seven of the eight amplifiers were removed, the noise floor was approximately one-half that of the normal signal-conditioning card configuration. One possible solution to the excessive noise floor problem would be to reduce the number of amplifier output reference lines that are tied together. In addition, unlike the Wheatstone bridge signal-conditioning card, the constant current loop signal-conditioning card does not have a filter after the amplifier. It was believed that this lack of a post-amplification filter was contributing to the high noise floor.

This theory was tested by routing the input of the data amplifier for a single gage measurement from the constant current loop signal-conditioning card to the input of the Wheatstone bridge measurement. This technique caused the constant current loop single gage output to be processed by the Wheatstone bridge circuitry which includes the data amplifier and an active low-pass filter. The results from this test are given in table 6.

Table 6. Constant current loop noise comparison test 3.

	Single gage output, Counts	Single gage output routed through the Wheatstone bridge signal path, Counts
Mean	2146	1877
Standard deviation	12	8

The noise floor level was reduced to approximately the same as the Wheatstone bridge when the output from the subtractor

19

was passed through the Wheatstone bridge gain amplifier, active low-pass filter, signal return, and PCM channel. It may be concluded, therefore, that the noise floor of the constant current loop signal-conditioning card would be significantly reduced by combining fewer signal returns and by placing a third-order, active, low-pass filter after the amplifier thus increasing the signal-to-noise ratio.

Future Testing

Before this constant current loop strain measurement system is used on future flight programs, additional tests should be performed. Such testing should include both laboratory and flight testing. The laboratory tests should include placing the test article under known mechanical and thermal loads and comparing the experimental data to analytical predictions. Additional flight testing should include performing loads maneuvers at supersonic speeds. This testing would enable the theoretical benefits of the constant current loop strain measurement system to be fully evaluated.

Concluding Remarks

The constant current loop strain measurement system provides strain measurements without the problem of reduced sensitivity caused by increasing lead wire resistance which is present with the Wheatstone bridge method. Additional benefits of the constant current loop method include the fact that the outputs from the constant current loop gages are approximately twice as large as the output from the Wheatstone bridge. The increased sensitivity of the constant current loop method can mitigate the reduction of gage output which results when the excitation voltage is lowered in the Wheatstone bridge system.

The in-flight evaluation of the constant current loop strain measurement method determined that the strains measured by the constant current loop compared well with the Wheatstone bridge measured strains. All three of the constant current loop wire configurations provided consistent results.

The seven-lead-wire configuration can read individual gage outputs which is typical of a rosette. However, corrections must be made for strain variations experienced by the individual gages of the seven-wire configuration because of differences between the resistances of the reference strain gage and the shock fence strain gages caused by temperature differences at the two locations.

The five-lead-wire configuration needs no assumptions made about the lead wire resistances. This configuration is insensitive to the temperature differences between the reference gage and the strain gages.

The benefit of the three-lead-wire configuration is that it uses only three lead wires, while the Wheatstone bridge requires four. Like the Wheatstone bridge method, the three-wire configuration can be susceptible to measurement errors caused by lead wire resistance changes. However, as long as the resistances of the two current-carrying lead wires change equally, the output is not affected. In the case of the Wheatstone bridge system, lead wire resistance increases reduce the sensitivity of the system to strain. The constant current loop five- and seven-wire configurations are not affected by increased lead wire resistances.

20

Two difficulties are currently being experienced with the constant current loop flight card system. The first is that the signal-to-noise ratio of the constant current loop signal-conditioning card is approximately the same as the Wheatstone bridge signal-conditioning card because the noise floor of the constant current loop signal-conditioning card is twice as high as the Wheatstone bridge. Constant current loop signal-conditioning card improvements, which are needed to reduce the noise level, include minimizing the number of reference lines tied together to the pulse code modulator and placing an active filter after the data amplifier. Once these improvements are made, the signal-to-noise ratio of the constant current loop system is expected to be twice that of the Wheatstone bridge.

In addition to improving the noise floor of the constant current loop signal-conditioning card, further testing should be performed before depending on this strain measurement system as the primary source of in-flight strain data.

APPENDIX A
WHEATSTONE BRIDGE AND
CONSTANT CURRENT LOOP CIRCUITS

Strain gages used in the Wheatstone bridges were configured into two four-active-arm-bending bridges. Figure A1 shows a generic diagram of the Wheatstone bridge containing four active gages with pairs acting in equal and opposite strain. The output voltage, V_{out}, is calculated using the following equation:

$$V_{out} = E(GF)(\varepsilon) \qquad (A1)$$

A detailed derivation of the Wheatstone bridge output is presented in reference 6.

The expected output from the constant current loop is derived using elementary circuit analysis to determine the voltage drop across the strain gages. The seven-wire configuration is used to read individual strain measurements across each gage of the bending bridge. Figure A2 shows the wiring schematic for the seven-lead-wire configuration. For explanation purposes, the output for gage 1 will be derived. Each gage in the bridge can be represented as a fixed resistance and a change in resistance caused by a strain input. Therefore, the voltage drop across gage 1 may be expressed by a constant current, I, multiplied by the sum of the resistance of gage 1, R_{g1}, and the change in that resistance, ΔR_{g1}, as shown in the following equation:

$$V_{g1} = I(R_{g1} + \Delta R_{g1}) \qquad (A2)$$

The R_{w2} and R_{w3} are not included in the equation because, theoretically, these terms may be neglected because of the high input impedance of the amplifier. In addition, any influence from the common mode voltage between the two leads would be minimized by the high common mode rejection ratio of the instrumentation amplifiers.
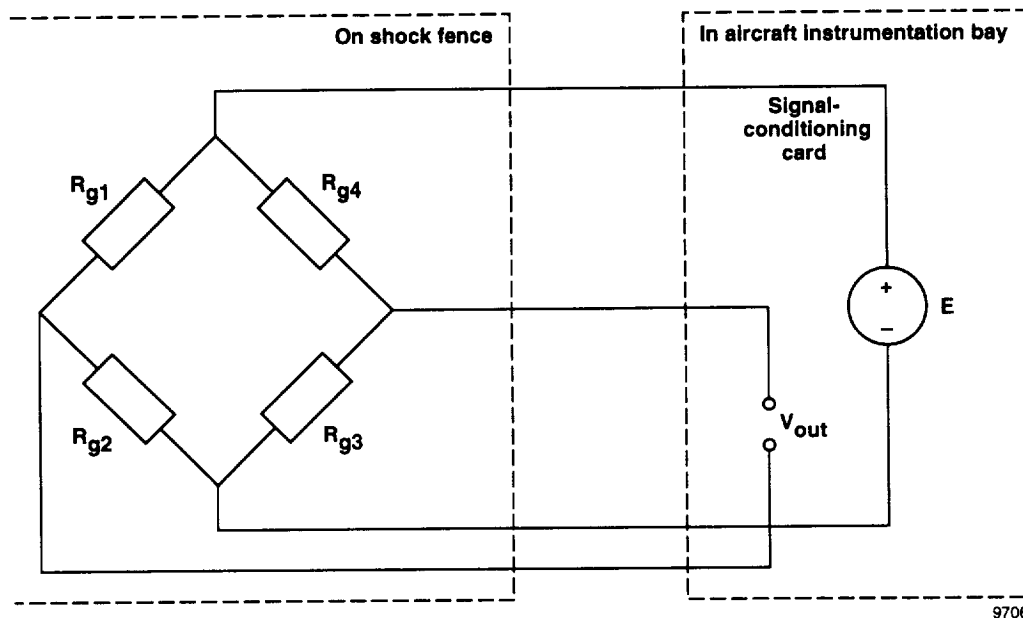

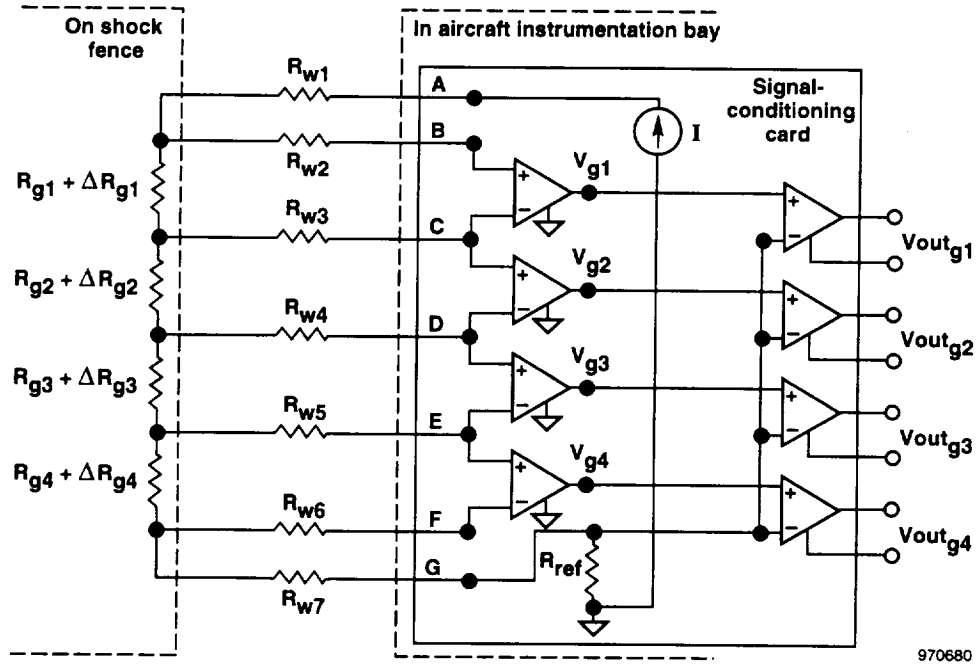Figure A1. A Wheatstone bridge configured in a four-active-arm-bending bridge.

22

Figure A2. Constant current loop seven-lead-wire configuration wiring diagram.

To obtain strain measurements, the voltage drop caused by the unstrained resistance, R_{g1} must be subtracted out. This subtraction is accomplished by placing a reference resistor R_{ref} in the current loop. The voltage drop across R_{ref} is subtracted from the output of the amplifier at V_a, and the output is expressed by:

$$V_{out_{g1}} = I(R_{g1} + \Delta R_{g1} - R_{ref}) \quad \text{(A3)}$$

The reference resistor is selected so that its resistance is equal to the gage resistance. The gage and reference resistance subtract out, and the output is simplified to

$$V_{out_{g1}} = I\Delta R_{g1} \quad \text{(A4)}$$

which is the output voltage due only to the change in resistance in gage 1.

The expected output from the five-lead-wire configuration is derived in a similar fashion as the seven-wire configuration. A diagram of the five-wire configuration is shown in figure A3. Lead wire resistances are denoted by R_w, and the gage resistances are represented by an unstrained resistance plus a change in that resistance, $R_g + \Delta R_g$, where ΔR_g results from a strain input. The V_a and V_b represent the voltage drops across both halves of the bridge. The voltage drops across V_a and V_b with a constant current source I, may be represented as in equations A5 and A6 by

$$V_a = I(R_{g1} + \Delta R_{g1} + R_{g2} + \Delta R_{g2}) \quad \text{(A5)}$$

$$V_b = I(R_{g3} + \Delta R_{g3} + R_{g4} + \Delta R_{g4}) \quad \text{(A6)}$$

The R_{w2}, R_{w3}, and R_{w4} may be neglected because of the negligible current
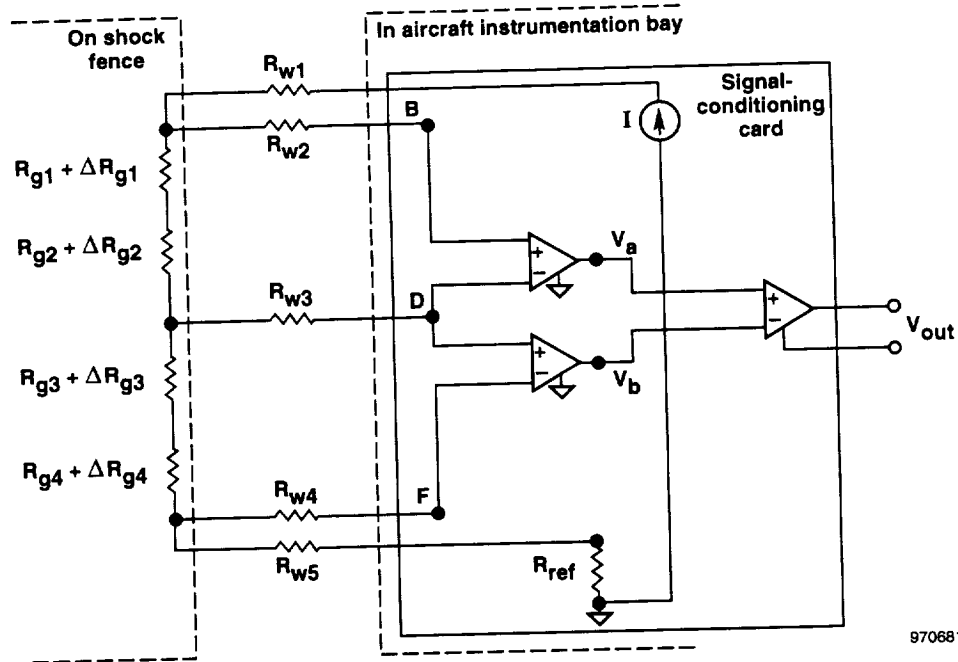
23

Figure A3. Constant current loop five-lead-wire configuration wiring diagram.

flow in these leads caused by the high input impedance of the instrumentation amplifier. Subtracting V_b from V_a yields the following voltage output:

$$V_{out} = V_a - V_b \qquad (A7)$$

Substituting in equations A5 and A6 for V_a and V_b, respectively, V_{out} becomes

$$V_{out} = I[(R_{g1} + \Delta R_{g1} + R_{g2} + \Delta R_{g2}) \\ - (R_{g3} + \Delta R_{g3} + R_{g4} + \Delta R_{g4})] \qquad (A8)$$

Assuming that all of the gages have the same initial resistance, V_{out} simplifies to

$$V_{out} = I[(\Delta R_{g1} + \Delta R_{g2}) \\ - (\Delta R_{g3} + \Delta R_{g4})] \qquad (A9)$$

where the output voltage is the difference between the strain gage pairs.

Like the five-lead-wire bridge, the three-wire configuration measures the output of four gages where gage pairs react to equal and opposite strain. The output voltage of this card is obtained by calculating V_a and V_b which are shown in the wiring diagram in figure A4.

Looking at the potential drop across the input of both amplifiers, the following equations for V_a and V_b are obtained:

$$V_a = I(R_{w1} + R_{g1} + \Delta R_{g1} \\ + R_{g2} + \Delta R_{g2}) \qquad (A10)$$

$$V_b = I(R_{w3} + R_{g3} + \Delta R_{g3} \\ + R_{g4} + \Delta R_{g4}) \qquad (A11)$$

Unlike the equation for the five-lead-wire configuration, R_{w1} and R_{w3} must appear in the equation because no sense leads are used to read the voltage across both
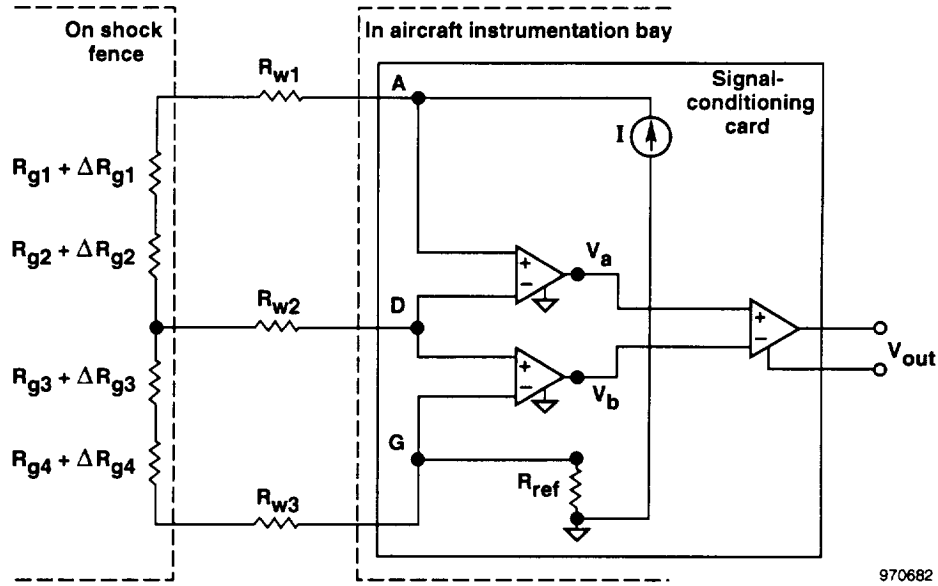
24

Figure A4. Constant current loop three-lead-wire configuration wiring diagram.

halves of the bridge. However, R_{w2} may be neglected because of the high input impedance of the amplifier and relatively small amount of current drawn into that lead wire. Subtracting V_b from V_a yields V_{out} in the following equation:

$$V_{out} = V_a - V_b \qquad (A12)$$

Substituting in equations A10 and A11, V_{out} becomes

$$V_{out} = I((R_{w1} + R_{g1} + \Delta R_{g1}$$
$$+ R_{g2} + \Delta R_{g2})$$
$$- (R_{w3} + R_{g3} + \Delta R_{g3}$$
$$+ R_{g4} + \Delta R_{g4})) \qquad (A13)$$

Assuming all of the R_g terms are equal, the R_g voltage drops cancel out, and equation A13 may be simplified to

$$V_{out} = I((R_{w1} + \Delta R_{g1} + \Delta R_{g2})$$
$$- (R_{w3} + \Delta R_{g3} + \Delta R_{g4})) \qquad (A14)$$

In the special case where all of the lead wires are the same length and the same temperature, it may be assumed that the lead wire resistances are equal and cancel out, and V_{out} is expressed by

$$V_{out} = I((\Delta R_{g1} + \Delta R_{g2})$$
$$- (\Delta R_{g3} + \Delta R_{g4})) \qquad (A15)$$

To obtain test data for the three constant current loop configurations, the five- and three-wire configurations were created from the seven-lead-wire output at the forward bridge location. The five-wire output was obtained on the signal-conditioning card by jumpering the voltages at the B, D, and F locations to other subtractor inputs. These jumpering locations are shown in figures A2 and A3. The three-wire configuration was created by jumpering the voltages at the A, D, and G locations to other subtractor inputs. These jumpering locations are shown in figures A2 and A4. The aft constant current loop gages were configured using the five-lead-wire configuration.

25

APPENDIX B
FLIGHT PROFILES

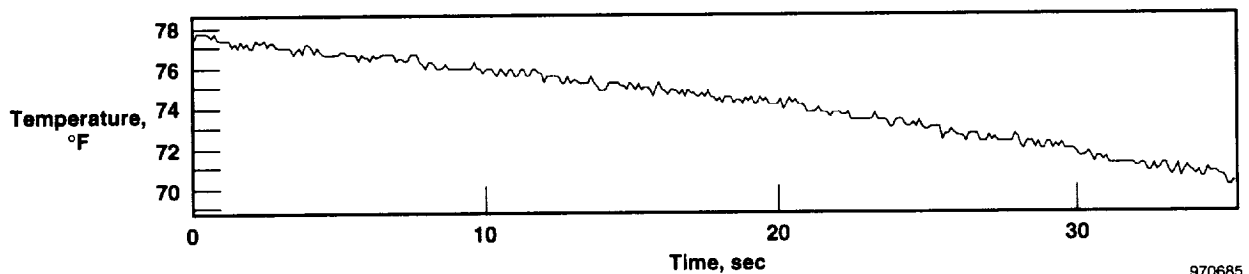Figures B1(a) through B1(e) and B2(a) through B2(e) show the Mach number, dynamic pressure, temperature, angle of attack, and angle of sideslip as a function of time for the maneuvers described in this document. These graphs illustrate the flight conditions which F-16XL ship 2 was experiencing when the strain measurements were taken.
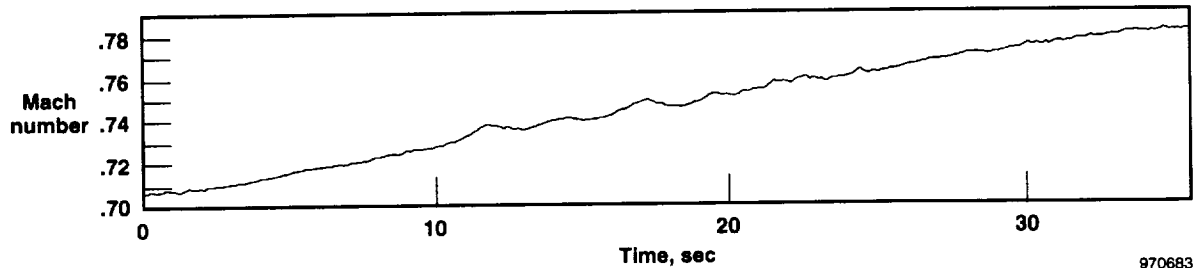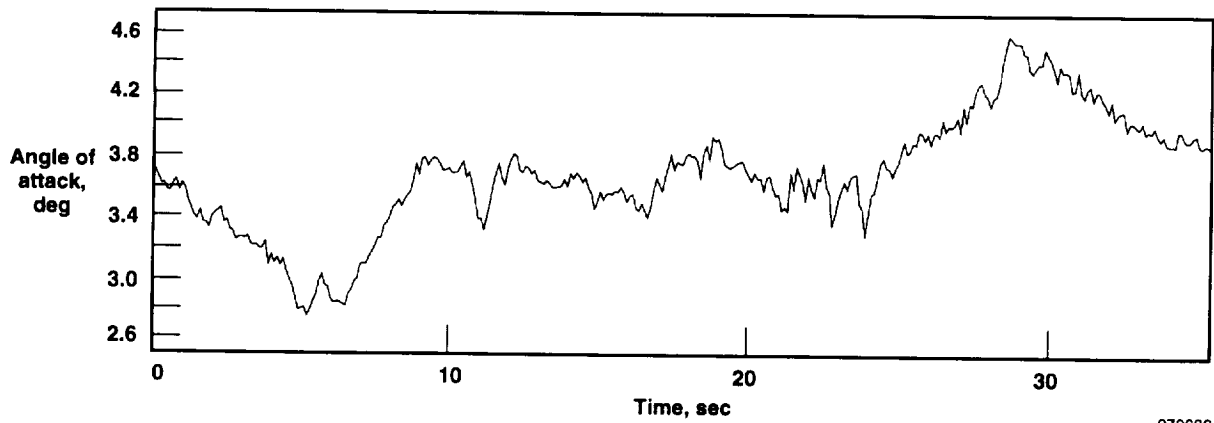

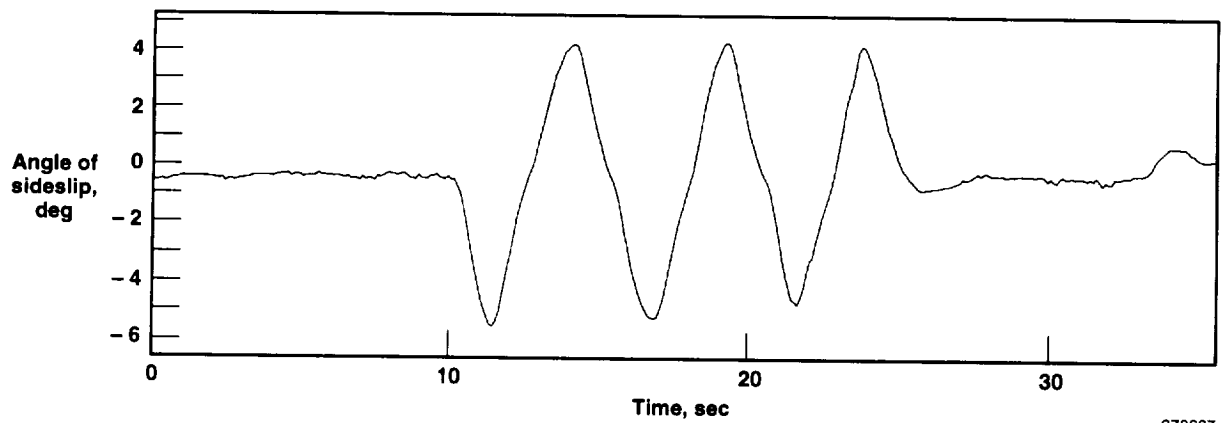(a) Mach number.
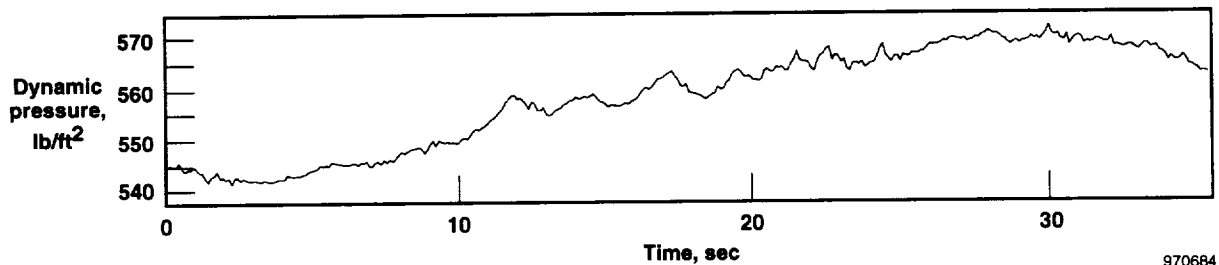
(b) Dynamic pressure.

(c) Shock fence temperature.

Figure B1. Flight parameters as a function of time during phasing maneuvers for flight 88.
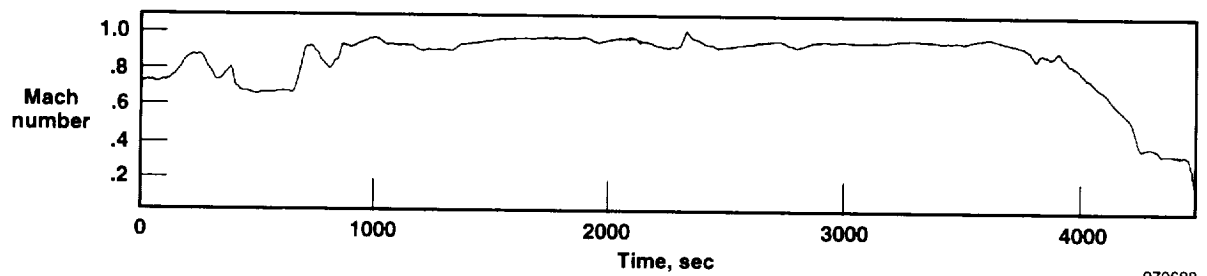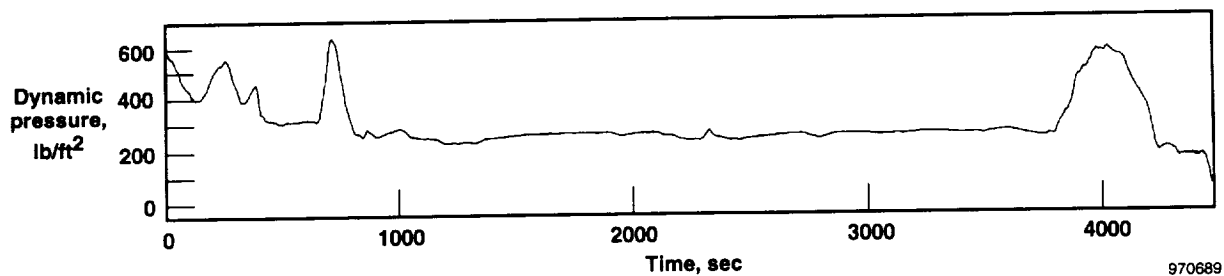
26

(d) Angle of attack.

(e) Angle of sideslip.

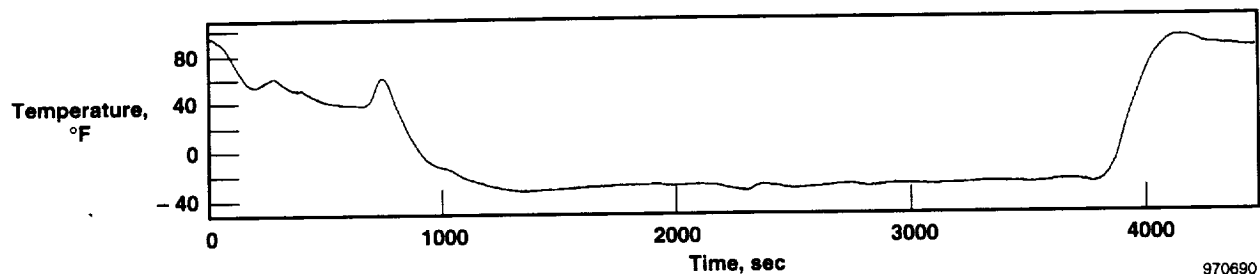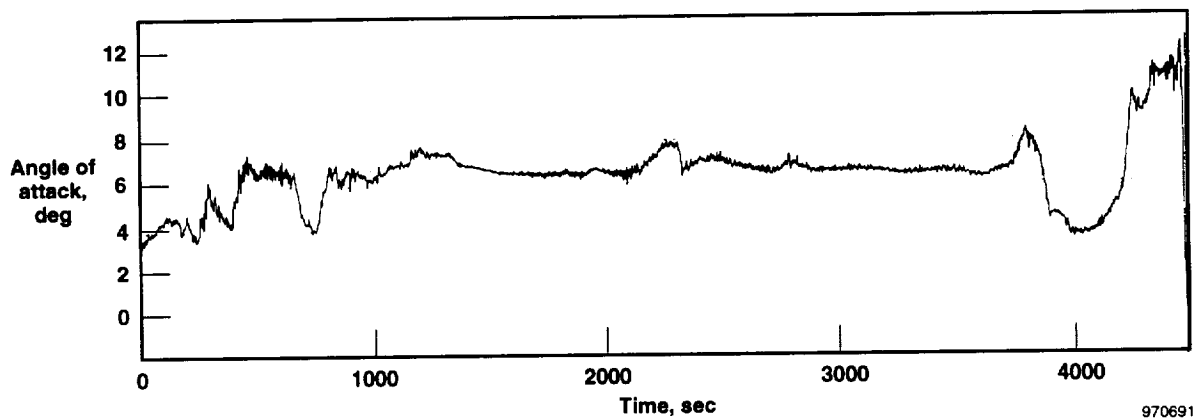Figure B1. Concluded.

(a) Mach number.

Figure B2. Flight parameters as a function of time during flight 87.
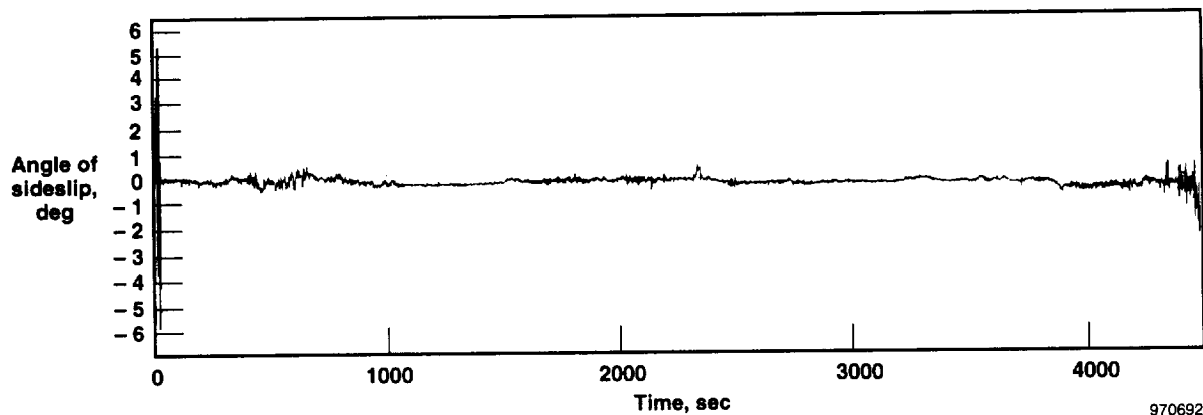
27

(b) Dynamic pressure.

(c) Shock fence temperature.

(d) Angle of attack.

(e) Angle of sideslip.

Figure B2. Concluded.

28

References

[1]Hannah, R. L. and Reed, S. E., ed., *Strain Gage Users' Handbook*, Elsevier Science Publishers Ltd., 1992, pp. 67–68.

[2]Anderson, Karl F., "Constant Current Loop Impedance Measuring System That Is Immune to the Effects of Parasitic Impedances," U.S. patent no. 5,371,469, Dec. 1994.

[3]Anderson, Karl F., *A Conversion of Wheatstone Bridge to Current-Loop Signal Conditioning for Strain Gages*, NASA TM-104309,1995.

[4]Anderson, Bianca T. and Bohn-Meyer, Marta, *Overview of Supersonic Laminar Flow Control Research on the F-16XL Ships 1 and 2*, NASA TM-104257, 1992.

[5]Dove, Richard C. and Adams, Paul H., *Experimental Stress Analysis and Motion Measurement*, Charles E. Merrill Books, Inc., 1964, pp. 117–124.

[6]Anderson, Karl F., *The Constant Current Loop: A New Paradigm for Resistance Signal Conditioning*, NASA TM-104260, 1992.

REPORT DOCUMENTATION PAGE

Public reporting burden for this collection of information is estimated to average 1 hour per response, including the time for reviewing instructions, searching existing data sources, gathering and maintaining the data needed, and completing and reviewing the collection of information. Send comments regarding this burden estimate or any other aspect of this collection of information, including suggestions for reducing this burden, to Washington Headquarters Services, Directorate for Information Operations and Reports, 1215 Jefferson Davis Highway, Suite 1204, Arlington, VA 22202-4302, and to the Office of Management and Budget, Paperwork Reduction Project (0704-0188), Washington, DC 20503.

1. AGENCY USE ONLY (Leave blank)	2. REPORT DATE	3. REPORT TYPE AND DATES COVERED
	August 1997	Technical Memorandum

4. TITLE AND SUBTITLE

A Limited In-Flight Evaluation of the Constant Current Loop Strain Measurement Method

5. FUNDING NUMBERS

WU 529-31-24

6. AUTHOR(S)

Candida D. Olney and Joseph V. Collura

7. PERFORMING ORGANIZATION NAME(S) AND ADDRESS(ES)

NASA Dryden Flight Research Center
P.O. Box 273
Edwards, California 93523-0273

8. PERFORMING ORGANIZATION REPORT NUMBER

H-2185

9. SPONSORING/MONITORING AGENCY NAME(S) AND ADDRESS(ES)

National Aeronautics and Space Administration
Washington, DC 20546-0001

10. SPONSORING/MONITORING AGENCY REPORT NUMBER

NASA TM-104331

11. SUPPLEMENTARY NOTES

Presented at the Society of Flight Test Engineers Conference, Orlando, Florida, August 18–22, 1997.

12a. DISTRIBUTION/AVAILABILITY STATEMENT

Unclassified—Unlimited
Subject Category 35

12b. DISTRIBUTION CODE

13. ABSTRACT (Maximum 200 words)

For many years, the Wheatstone bridge has been used successfully to measure electrical resistance and changes in that resistance. However, the inherent problem of varying lead wire resistance can cause errors when the Wheatstone bridge is used to measure strain in a flight environment. The constant current loop signal-conditioning card was developed to overcome that difficulty. This paper describes a limited evaluation of the constant current loop strain measurement method as used in the F-16XL ship 2 Supersonic Laminar Flow Control flight project. Several identical strain gages were installed in close proximity on a shock fence which was mounted under the left wing of the F-16XL ship 2. Two strain gage bridges were configured using the constant current loop, and two were configured using the Wheatstone bridge circuitry. Flight data comparing the output from the constant current loop configured gages to that of the Wheatstone bridges with respect to signal output, error, and noise are given. Results indicate that the constant current loop strain measurement method enables an increased output, unaffected by lead wire resistance variations, to be obtained from strain gages.

14. SUBJECT TERMS

Circuit theory, Constant current loop, F-16XL aircraft, Strain gage, Structural testings, Wheatstone bridge

15. NUMBER OF PAGES

33

16. PRICE CODE

AO3

17. SECURITY CLASSIFICATION OF REPORT	18. SECURITY CLASSIFICATION OF THIS PAGE	19. SECURITY CLASSIFICATION OF ABSTRACT	20. LIMITATION OF ABSTRACT
Unclassified	Unclassified	Unclassified	Unlimited

NSN 7540-01-280-5500